Turbulence Modeling of a Small Quadrotor UAS Using System Identification from Flight Data

Ondrej Juhasz   **Mark J.S. Lopez**
Research Associate   Research Associate
San Jose State University
Ames Research Center
Moffett Field, CA

Marcos G. Berrios   **Tom Berger**   **Mark B. Tischler**
Aerospace Engineer   Aerospace Engineer   Senior Scientist
U. S. Army Aviation Development Directorate (AMRDEC)
Ames Research Center
Moffett Field, CA

ABSTRACT

The extraction of a turbulence model for a small quadrotor UAS using flight test data is presented and validated using simulation. The turbulence model is a control equivalent turbulence input (CETI) model, which drives the controls of the aircraft to reproduce realistic motion caused by turbulence. Since the quadrotor UAS is unstable, the extraction methodology must be done with a control system engaged. Effects of signal length, noise in the feedback path, and model uncertainty on the extraction methodology are quantified in simulation and recommendations are given to obtain high quality flight test data for accurate extraction of turbulence models. The extracted turbulence model is shown to have the same low-order form as existing turbulence models.

NOTATION

Symbols

G_c	Control system
G_{δ_t}	CETI Transfer function
G_{xx}	Signal autospectrum, plotted in power dB; $10\log 10\,|G_{xx}|$
J	Model Cost: Error of fit between model and truth data
q_a	Acutal aircraft pitch rate (rad/sec)
q_m	Measured pitch rate (rad/sec)
δ_a	Bare-airframe input (mixer units: +/- 4500)
δ_c	Commanded input (mixer units)
δ_l	Commanded rate response (rad/sec)
δ_t	Turbulence input (mixer units)
η	Noise (units of bare-airframe output)
$\bar{\sigma}_{q_m}$	Signal-to-noise ratio
τ	Time delay (seconds)

Acronyms

ADD	Aviation Development Directorate
GNC	Guidance Navigation and Control
CETI	Control Equivalent Turbulence Input
PSD	Power Spectral Density

INTRODUCTION

The popularity of small unmanned aerial systems (UAS) has continued to increase in both the military and commercial markets. For the military, small VTOL UAS offer the ability to dramatically increase the warfighter's situational awareness on the battlefield, while commercially they may deliver packages or medicine to a company's customers. Quadrotors in particular have become popular due to their mechanical simplicity over traditional single main rotor helicopters that have swashplates.

Due to the low cost of the aircraft themselves, small UAS are generally developed with a "fly-crash-fix" cycle, where engineering design and analysis methods may be overlooked in favor of quickly getting in the air. However,

as the technology contained in a UAS becomes more advanced and the acquisition process becomes more rigorous, properly vetted engineering methods will need to be utilized. For example, more emphasis will need to be placed on the control system design and validation effort.

System identification has long been used to develop accurate bare-airframe models of fixed- and rotary-wing aircraft (Refs. 1, 2). These identified models are often used as the basis for control law design and development, especially when physics-based models are not available or reliable. Recently, frequency-domain system identification methods have successfully been demonstrated on quadrotors in hover/low-speed flights (Refs. 3, 4). Low-order state-space models are fit to the frequency responses to get an accurate representation of aircraft dynamics over a broad frequency range. The identification results show that small VTOL UAS have unstable modes that are at much higher frequency than manned size VTOL and require high-bandwidth control systems to stabilize them.

Control systems for these UAS must provide good stability characteristics, closed-loop tracking performance, and disturbances rejection capabilities. Realistic turbulence models are important for successfully designing and validating controller disturbance rejection performance in a simulation environment. The Dryden turbulence model represents turbulence based on a "frozen-field" through which the helicopter flies through. This type of model is very common in fixed wing aircraft, but is not applicable to hovering flight. Therefore, a turbulence model based on the control equivalent turbulence inputs (CETI) is developed (Refs. 5, 6). The CETI model uses flight data taken in turbulence to reproduce control inputs needed to generate the same levels of motion as were seen during the flight in turbulence. The extraction process requires an accurate model of the bare-airframe. While applied differently, both the CETI and Dryden turbulence models capture low-order representations of turbulence. Within control design, a similar approach to the CETI model has been successfully used to generate the required inputs to negate the effects of disturbances based on estimated control equivalent disturbance inputs (Ref. 7).

This paper will outline a frequency-domain based CETI model extraction methodology and apply it to data extracted from time histories taken in flight in turbulence. The extraction methodology will first be validated in simulation by investigating the effects of time history length, sensor signal-to-noise ratio, and quadrotor bare-airframe uncertainty. It will be shown that an accurate CETI model can be extracted from the given time-history data, and that the extracted CETI model in simulation exactly reproduces the model derived from flight.

The work in this paper falls under the Aviation Development Directorate (ADD) Quadrotor Guidance, Navigation, and Controls (GNC) Project (Ref. 8). This project aims to adapt the state-of-the-art modeling, guidance, and controls technologies and methodologies used at ADD for large-scale vehicles to small-scale UAS.

QUADROTOR AIRCRAFT DESCRIPTION

The aircraft used is the 3DR Iris+ (herein Iris) quadrotor shown in Fig. 1. The Iris weighs about 2.6 lbs, has four twin bladed 10 inch propellers, and uses a Pixhawk flight control processor, which runs the opensource Ardupilot codebase. This software provides all sensor processing and flight control, and runs at 400 Hz. The base code was modified to include additional logging to track inputs going into the mixer. All logging data is generated at 200 Hz. The ability to add inputs directly to the mixer was also incorporated. Direct mixer inputs were used during the bare-airframe identification process to excite the bare-airframe response of the quadrotor without the filtering of the control system.
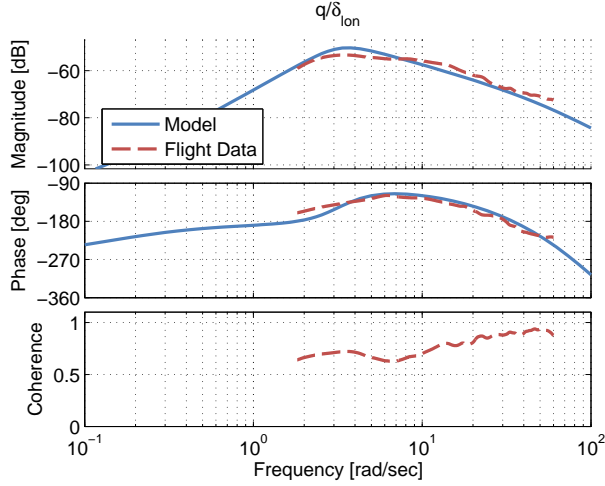

Fig. 1. 3DR Iris+ quadcopter

Bare-Airframe System Identification

As part of the ADD Quadrotor GNC project, the frequency-domain based system identification tool, CIFER® (Ref. 1), was used for both the state-space model identification, as well as the generation of autospectra of CETI time histories presented here.

The Iris longitudinal dynamics are dominated by an unstable mode between $\omega = 3 - 4$ rad/sec (Fig. 2). In order to stabilize this mode, the crossover frequency in this axis must be significantly higher, and it is near $\omega = 30$ rad/sec in the stock control system. This need for a high crossover frequency drives the need to have an accurate model up to at least 60-90 rad/sec (Ref. 1) for control system design.

The bare-airframe identification model structure and results align well with those previously published (Refs. 3, 4). A total of 15 states were required to model the full aircraft, including the 9 rigid-body states as well as high-frequency "lags". The lags represent high-frequency roll off in magnitude and phase that can be attributed to motor dynamics, structural dynamics, and on-board sensor filtering. A time-delay was also used in each axis that accounts for sensor and processing delays.

The identified longitudinal dynamics are overlaid with flight data in Fig. 2. The state-space longitudinal dynamics

Fig. 2. Hover pitch rate response to longitudinal mixer inputs

Table 1. Iris Longitudinal Identification Results

Engineering Symbol	Value	CR (%)	Insens. (%)
$M_{\delta_{lon}}$	0.01362	3.62	1.36
X_u	-0.1428	7.32	2.53
M_u	1.102	6.90	2.14
M_q	0.000	-	-
lag[a]	50.0	-	-
τ	0.02811	6.47	3.22

[a] Fixed parameter
[b] Eliminated parameter

Fig. 3. Simplified block diagram of aircraft pitch rate response including turbulence inputs

equations in hover are shown in Eqn. (1) and the parameters are given in Table 1, along with their Cramer-Rao bounds and insensitivities (Ref. 1). The implementation of the lag puts the control derivative ($M_{\delta_{lon}}$) in the A matrix, which is now driven by the lagged control input, δ'_{lon}. All parameters are well identified with low Cramer-Rao bounds and insensitivities, giving a high confidence in the physical parameters of the model. The pitch rate damping derivative (M_q) was found to have a negligible influence on the model and was eliminated from the identification. Excellent fits to flight data were also obtained for the lateral, direction, and heave axes. This paper will demonstrate the CETI extraction method on the longitudinal axis, so figures are included for that axis only. The average cost of the identification for all axes, $J_{ave} = 43$, is is well below the $J_{ave} \leq 100$ threshold (Ref. 1), meaning an excellent fit has been obtained.

$$\begin{Bmatrix} \dot{u} \\ \dot{q} \\ \dot{\theta} \\ \dot{\delta'}_{lon} \end{Bmatrix} = \begin{bmatrix} X_u & 0 & -32.174 & 0 \\ M_u & M_q & 0 & M_{\delta_{lon}} \\ 0 & 1 & 0 & 0 \\ 0 & 0 & 0 & -lag \end{bmatrix} \begin{Bmatrix} u \\ q \\ \theta \\ \delta'_{lon} \end{Bmatrix}$$
$$+ \begin{bmatrix} 0 \\ 0 \\ 0 \\ lag \end{bmatrix} \{\delta_{lon}(t - \tau)\} \quad (1)$$

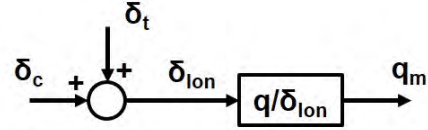### CETI EXTRACTION

Extraction Methodology

Since the Iris bare-airframe is highly unstable, all turbulence data must be collected with the control system engaged. The baseline Iris control system called "Stabilize" mode provides attitude stabilization. Once in a hover, the aircraft was kept in roughly the same location but was allowed to drift to minimize additional inputs into the control system. Long time histories were used to ensure the aircraft was adequately perturbed and to capture low frequency dynamics. The use of closed-loop responses is in contrast to the results in (Ref. 5), where only time histories in which aircraft motion was uncorrelated with pilot inputs were used. This meant the pilot input (δ_c) was uncorrelated with the reconstructed bare-airframe input (δ_{lon}) and that the aircraft motion was coming purely from excitation by turbulence.

The turbulence extraction and identification methodology aims to identify an equivalent control input (δ_t) which excites the aircraft similarly to real turbulence. This is the same approach used in Ref. 5. The concept is shown in Fig. 3 for the longitudinal axis, where the measured aircraft response (q_m) is driven by the commanded inputs (δ_c) as well as turbulence inputs (δ_t). In equation form the total measured pitch rate is:

$$q_m = \frac{q}{\delta_{lon}}(\delta_c + \delta_t) \quad (2)$$

Solving for the turbulence input gives:

$$\delta_t = \frac{\delta_{lon}}{q}q_m - \delta_c \quad (3)$$

Measured aircraft rates are passed through the inverse of the identified aircraft model, reconstructing the control inputs needed to generate the rates. Measured commanded inputs are then subtracted from these inputs, leaving control equivalent turbulence inputs. The results generated here are solely in the frequency domain, so a "stabilized inverse" is not required, as was in Ref. 5, which used a time-domain

approach to reconstruct the bare-airframe inputs. In the frequency domain, the arithmetic of Eqn. (3) (using a linear, not logarithmic scale) is (Ref. 9):

$$G_{\delta_t \delta_t} = \left| \frac{\delta_{lon}}{q} \right|^2 G_{q_m q_m} - G_{\delta_c \delta_c} \qquad (4)$$

VALIDATION OF THE CETI EXTRACTION METHOD USING SIMULATION

The block diagram in Fig. 3 is valid for an open-loop system where there is no effect of feedback. Since the CETI extraction process was done on a closed-loop system, it is important to understand the effects of sensor noise and plant modeling uncertainty on the resulting model. It is known that for good signal-to-noise ratios, the bare-airframe model extracted from closed-loop simulation is unbiased for output measurement noise (Ref. 1), but the effect of measurement noise on the CETI model extraction is unclear. It is also important to investigate the required signal lengths. In order to get adequate low frequency data, long time histories may be needed, and the exact length is unknown. An analysis was conducted on a closed-loop simulation of an Iris in order to clarify the effects of:

- Signal length

- Measurement noise

- Bare-airframe model uncertainty

Simulation Setup

The simulation model is shown in Fig. 4 and contains the closed loop longitudinal axis attitude-hold dynamics similar to the stock Iris. In order to provide a realistic model of the Iris, the simulation uses the longitudinal dynamics from the identified state-space Iris model ($H = q/\delta_{lon}$) from Fig. 2 and a control system (G_c) which has a similar crossover frequency to the stock "Stabilize" mode used in the flight test. The CETI model used is a low-order turbulence model (Eqn. 5) where the gain (K) and break frequency (a) were set to generate meaningful levels of turbulence in the simulation and to be consistent with results in Ref. 5. The CETI model is driven by a white noise (w_n) signal and the resulting turbulence input (δ_t) enters the system at the mixer and sums with the commanded inputs from the control system (δ_c) to form the aircraft bare airframe input (δ_{lon}). The aircraft pitch rate (q) is summed with sensor noise (η) to form the total measured pitch rate (q_m) which is used in the feedback. Pilot and outer loop control inputs (δ_l) are assumed to be small and uncorrelated with the turbulence and noise and so should not have a large effect on the extracted CETI model.
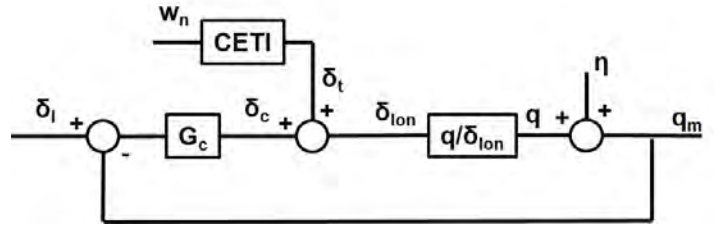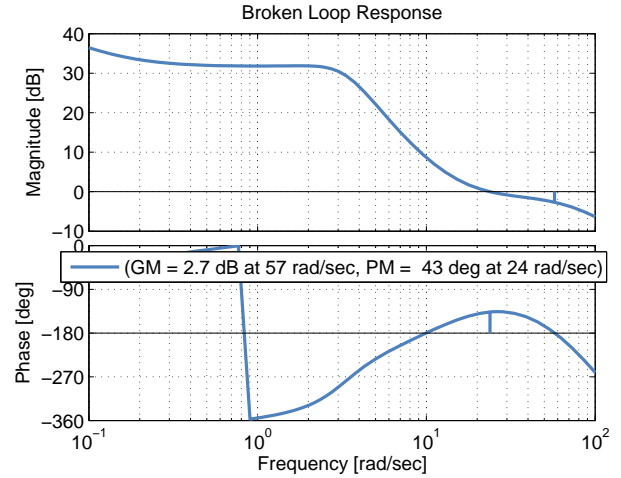

Fig. 4. Block diagram of simulation dynamics

Fig. 5. Simulation broken loop response

$$G_{\delta_t}(s) = \frac{K}{s+a} \qquad (5)$$

The broken loop response for the loop broken at the actuators ($G_c H$) is shown in Fig. 5. Also shown are the control system crossover frequency and stability margins. This control system has been tuned to have a high disturbance rejection bandwidth and a crossover frequency similar to the stock Iris. Details of the controller optimization process are given in Ref. 10.

Baseline CETI Model Extraction

The baseline model extraction uses the arithmetic in Eqn. (4) to re-identify a known CETI model using an exactly known plant and CETI model with no sensor noise and so represents a best case scenario. Time signals of 300 seconds were used to align the extraction with signal lengths obtained in flight. The autospectra of the truth CETI model and PSD as well as the extracted CETI model are shown in Fig. 6. The truth CETI PSD curve represents the PSD of the truth CETI model (Eqn. 5) using the 300 second generated white noise signal. The extracted CETI model (using Eqn. (4)) aligns nearly exactly with the truth CETI PSD at low freqeuncies up to $\omega = 7$ rad/sec, validating the extraction in perfect conditions. The extraction process then oscil-
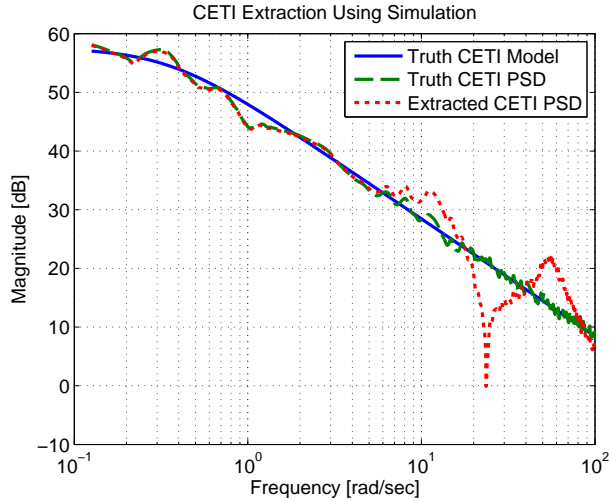
Fig. 6. Extraction of CETI model using simulation

Fig. 7. Component signal PSDs used to generate CETI response
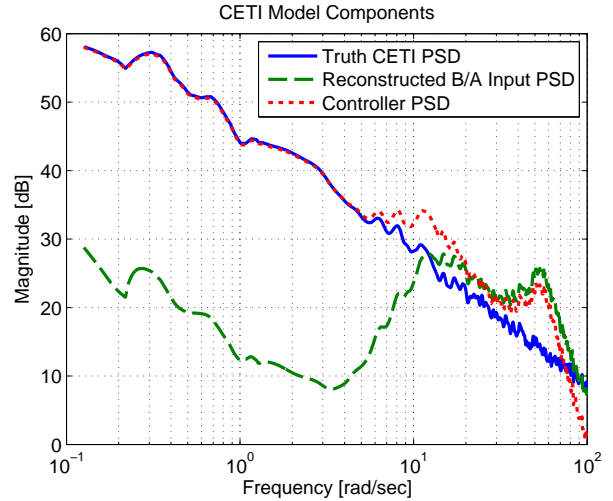
lates around the true response at frequencies near the control system crossover. Well above crossover (not shown), the extracted CETI response aligns again with the truth data.

The CETI turbulence is obtained by subtracting the mixer input (δ_c) from the reconstructed bare-airframe input (δ_{lon}), both of which are plotted in Fig. 7. The controller input dominates at low frequency up to about $\omega = 5$ rad/sec, and the reconstructed bare-airframe input is nearly two orders of magnitude (30 dB) lower. At these frequencies, the aircraft does not move and the control system takes out all turbulence through the feedback of pitch rate. The mixer input is exactly opposite of the CETI turbulence input. At $\omega > 5$ rad/sec, the broken loop response (Fig. 5), shows a dramatic drop; the control system is becoming less effective at removing turbulence and the aircraft begins to move. Signal autospectra contain only magnitude information, so the relative phasing of the control system input and bare-airframe input signals are not known, and the extraction process breaks down. At frequencies much higher than crossover (not shown), the control system is ineffective and the turbulence input directly drives aircraft motion, and the CETI model is again cleanly extracted from the data.

This simple analysis shows that if the crossover frequency is high enough, the CETI model is able to be cleanly identified using the extraction process.

Length of Required Flight Data

White noise has a PSD of unity across all frequencies and for infinite time scales. However, the PSD at low frequency for short signal lengths might not equal exactly one. This section identifies the signal durations necessary to accurately identify low frequency dynamics when driven in the time domain by white noise. White noise is driven through the CETI model from Eqn. (5) and the corresponding PSDs ($G_{\delta_t \delta_t}$) are shown in Fig. 8 for a range of time histories between 100 to 1200 seconds. For short time histories, the
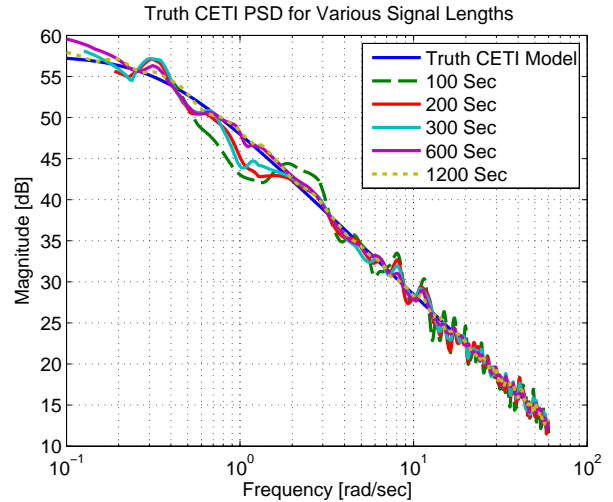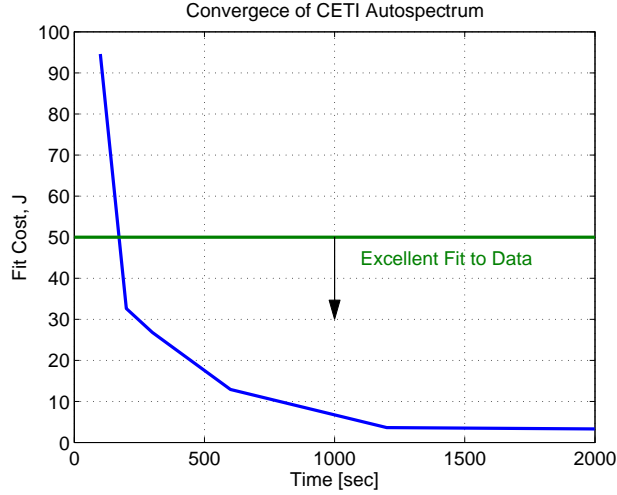

Fig. 8. PSD of white noise of different lengths being passed through CETI model

PSD at low frequency shows considerable variability from the truth data, and the PSD converges on top of the model for very long time histories.

The cost based on the error between the autospectrum of the time signals and the model (see Ref. 1) is shown in Fig. 9. As the signal length increases, enough averages of the white noise are achieved and the cost approaches 0, an exact fit to the model. Guidelines from Ref. 1 indicate a cost of less than 50 gives an excellent match to truth data. For the turbulence to achieve a good fit to the model, more than 200 seconds of data are required. This indicates that the Iris must be flown for at least 200 seconds in a turbulence field to achieve adequate spectral content to extract an accurate CETI model. The time histories obtained in turbulence in flight meet this criteria.

Fig. 9. Cost of fit between white noise of different lengths being passed through CETI model and the exact CETI model

Convergence of Autospectra

The simulations are driven by random white-noise processes. If time histories are generated with different noise seeds, they will form slightly different autospectra. This is true for flight data as well, as different time histories taken right after one another will have different spectral content. Figure 10 shows the band within which the real turbulence model will fall into when driven by 300 seconds of white noise with different noise seeds.

CIFER® can average multiple time histories to produce a single autospectrum (Ref. 1). As the number of time histories used increases, they will average to produce the exact CETI turbulence model. The cost decreases from $J = 20$ to 6 just by using two, 300 second time histories. Two time histories were obtained for all flights in turbulence, so an excellent representation of the CETI dynamics should be extracted from the flight data.

Influence of Measurement Noise

In a closed-loop system, measurement noise is correlated around the loop and may be amplified, degrading the accuracy of the extracted CETI model. To better understand the affects of output noise, various levels of measurement noise (η) are added to the system in Fig. 4 and the resulting models are overlayed with each other. In transfer function form, the effect of measurement noise on the measured bare-airframe output signal as shown in Fig. 4 is:

$$q_m = -\frac{1}{1 + G_c H}\eta + \frac{H}{1 + G_c H}\delta_t \qquad (6)$$

Solving for the turbulence input:

$$\delta_t = \frac{1 + G_c H}{H}q_m + \frac{1}{H}\eta \qquad (7)$$
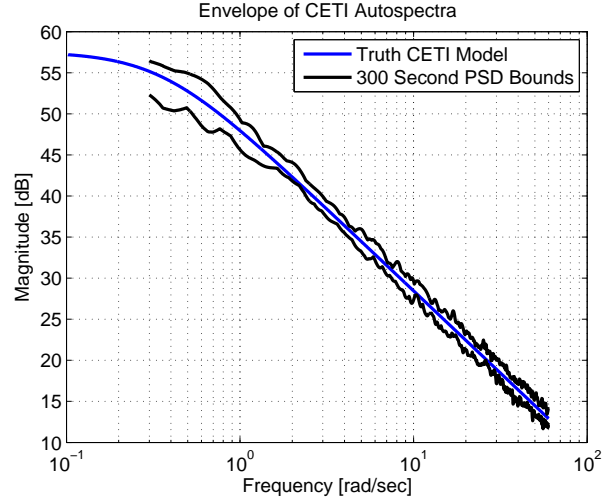
Fig. 10. Envelope of upper and lower bounds of CETI autospectra that may be obtained from different time histories

The two components that characterize the predicted turbulence are the measured rate (q_m) as well as noise (η), both easily measurable in this simulation case. Figure 11 shows the magnitude component of the two transfer functions from Eqn. (7) that multiply the measured pitch rate and noise input, respectively. At frequencies well below crossover ($\omega = 24$ rad/sec), the noise signal is attenuated by nearly 40 dB when compared to the pitch rate signal. At these frequencies, noise will have a small impact on the extraction of the CETI model. Near and above crossover, the noise signal is the same as, or amplified more than, the measured rate signal, meaning an accurate representation of turbulence will not be obtained at these frequencies if there is high signal to noise. This simple analysis demonstrates that for a closed loop CETI extraction, a high bandwidth control system is needed as reasonable results cannot be expected above crossover frequency if there is any noise in the measurements.

To provide further insight, the simulation in Fig. 4 was run for 300 seconds with varying levels of sensor noise. Based on the results from Fig. 9, this signal length should allow for excellent identification results close to the known CETI model. Noise levels were chosen to give a broad range of signal-to-noise ratio, defined as the the signal root-mean-square (RMS) value divided by the noise RMS value. Large signal-to-noise ratios signify high quality, low noise data.

Figure 12 shows PSDs of the varying simulated measurement noise levels plotted along with the simulated measured aircraft rates, q_m. At low frequencies below crossover, all aircraft rates align well with each other and the no noise case. The noise is well attenuated by the control system when compared to turbulence inputs, as predicted by Fig. 11, and the simulated measured rate does not change. At around $\omega = 10$ rad/sec for the highest noise
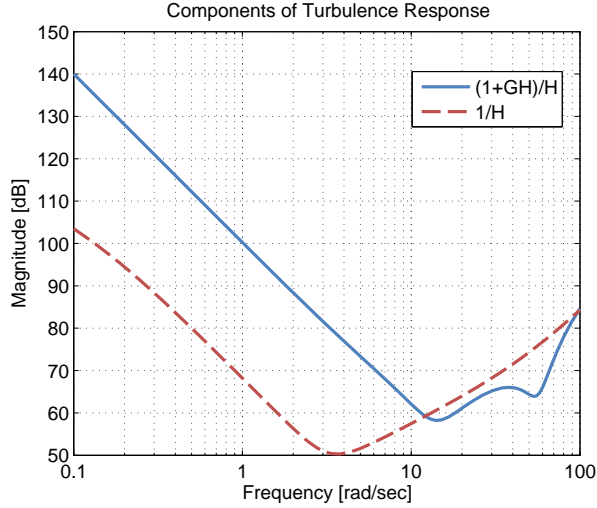
Fig. 11. Frequency responses comparing the scaling of measured output and measurement noise on CETI extraction

case, the measured response begins to be fully dominated by the noise and the control system is becoming ineffective at removing it. Well above crossover, the noise is directly fed into the measured rate for all cases.

Figure 13 shows the extracted CETI model for the varying measurement noise cases as well as the truth CETI model and PSD signal. It is clear that as the signal-to-noise ratio increases, the CETI extraction procedure breaks down. This figure also clearly shows where the identification of the CETI model from flight data would need to take place and that a max frequency of about 10 rad/sec should be used in the identification.

The CETI costs are determined by using the autospectra of the extracted CETI model and the truth CETI model and are plotted in Fig. 14. The costs is determined between $\omega = 0.4$ and 10 rad/sec (beyond which CETI extraction breaks down). Minimum signal-to-noise ratios of $\bar{\sigma}_{q_m} = 2.5$ are needed in order to accurately extract a model from turbulence. This is consistent with recommended signal-to-noise ratio $\bar{\sigma}_{q_m} > 3$ that is needed to accurately ($< 10\%$ bias error) extract a bare-airframe model from a closed loop response (Ref. 1).

To quantify the signal-to-noise ratio from flight data, two time histories taken during flight in turbulence were analyzed. Two additional time histories taken from indoor flights were also analyzed, where the turbulence was characterized as minimum. The measured pitch rate autospectra are shown in Fig. 15. Ref. 11 defines the signal-to-noise ratio from flight data ($\bar{\sigma}_{q_m}$) as a ratio of the RMS of two portions of the autospectrum. The autospectrum is assumed to be noise once it plateaus at high frequency. This plateau occurs at $\omega = 30$ rad/sec for the data in Fig. 15 and an additional on-board filter around $\omega = 50$ rad/sec filters the noise
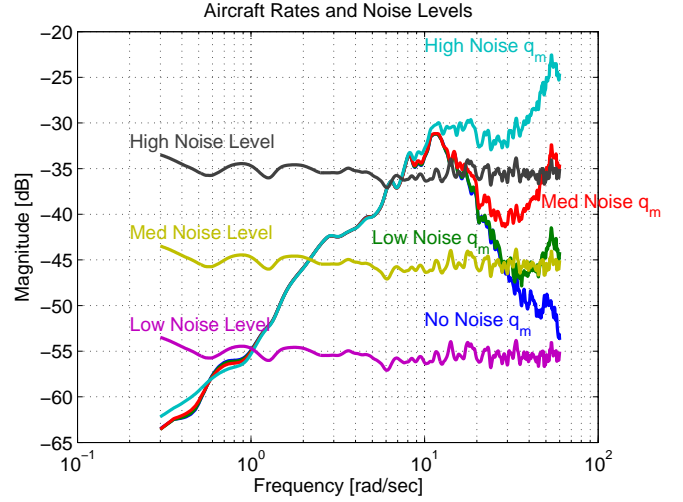
Fig. 12. Measured aircraft rates with increasing measurement noise levels
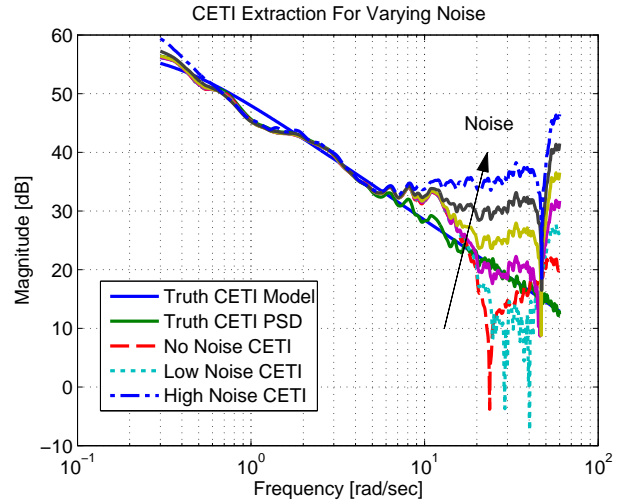
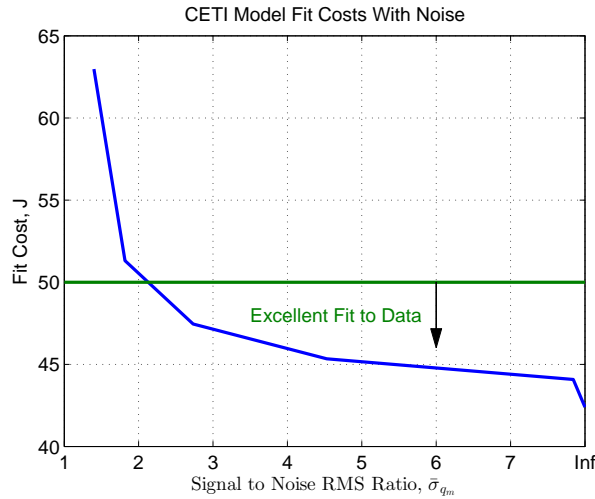Fig. 13. Extracted CETI models with varying measurement noise

out completely. The autospectrum is considered to be signal at frequencies below the noise plateau.

Following this analysis, the flight data for the Iris has a signal to noise ratio of $\bar{\sigma}_{q_m} = 2.6$ for the outdoor data and a better $\bar{\sigma}_{q_m} = 3.9$ for the indoor data. Based on Fig. 14, the Iris data is adequate for accurate extraction of the CETI model.

Bare-Airframe Uncertainty

Variability of the bare-airframe model could also impact the CETI extraction. The exact Iris dynamics are not known. The identified state-space model parameters have Cramer-Rao bounds, which give a measure of 1σ uncertainty of the parameters. In the proceeding analysis, each parameter is varied by $\pm 2\sigma$ to capture a 95% probability of capturing

Fig. 14. Extracted CETI model cost changes with varying signal-to-noise ratio, $\bar{\sigma}_{q_m}$
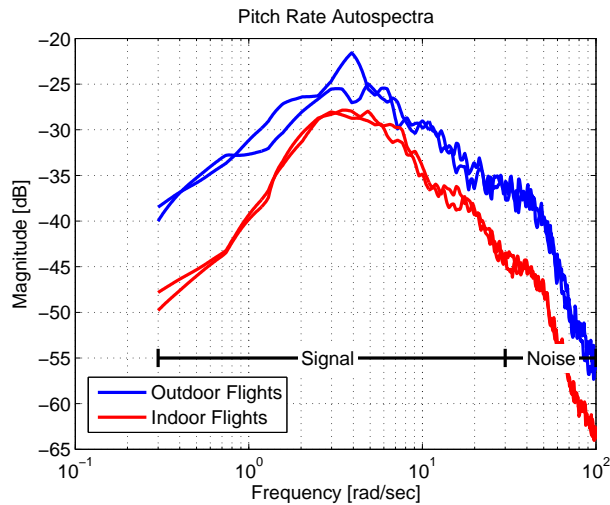
Fig. 15. Pitch rate autospectra from flight used to measure signal-to-noise ratio

the correct value of the parameter. This is done for all possible combinations of parameters from Table 1. Time histories of 300 seconds are used, as is a signal-to-noise ratio of $\bar{\sigma}_{q_m} = 2.6$, to closely match the Iris flight data. The CETI extraction method remains the same for each case. The nominal bare-airframe model is used for the inverse in Eqn. (4). The resulting CETI models are plotted along side the truth data in Fig. 16. The parameters from Table 1 are relatively well identified, with Cramer-Rao percentages generally below 7%, so large changes to the extracted CETI model were not anticipated between the original and perturbed results. The cost of fitting the perturbed models did not vary by more than $\Delta J = 5$ from the cost of fitting the original extracted CETI model.

Since the bare-airframe model is well identified, it is not anticipated that uncertainty will have an impact the CETI extraction using flight data.
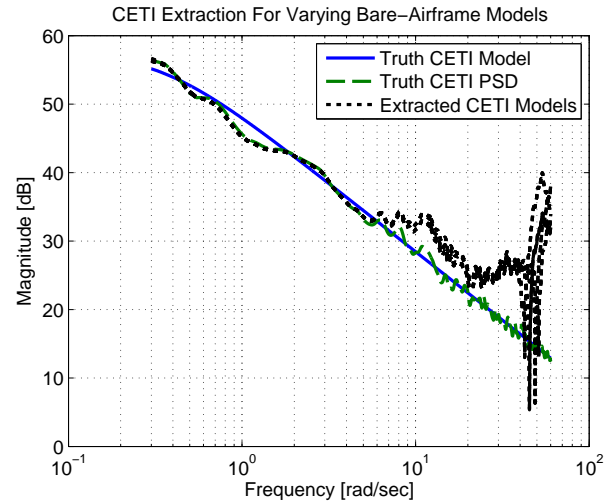
**Fig. 16. Effect of bare-airframe 2σ uncertainty on the extracted CETI model**

Guidelines

The simulation model of the Iris was used to validate the extraction methodology and develop requirements for accurate CETI extraction from flight. These guidelines are as follows:

1. Around crossover, the CETI extraction process breaks down. It is important that the control system crossover either be sufficiently high (around $\omega = 30$ rad/sec), or the flights in turbulence are done with the controller off and the pilot stabilizes the vehicle with small inputs.

2. Time histories of at least 200 seconds are required to provide adequate spectral content at low frequency.

3. Signal-to-noise ratios of $\bar{\sigma}_{q_m} > 2.5$ are needed to provide clean data with low CETI model extraction costs.

4. Bare-airframe uncertainty was not shown to have a large impact. However, all parameters in the state-space model were accurately identified and the resulting model matched well with the non-parametric frequency response. If an accurate model is not know there will certainly be effects on the CETI extraction.

CETI MODEL EXTRACTION USING FLIGHT DATA

Time histories taken in the same turbulence level were processed to determine the equivalent turbulence input using Eqn. (4). An anemometer was not available during the testing, so the exact variation in wind-speeds is not know. The resulting extracted CETI autospectrum is shown in Fig. 17, along with a corresponding first-order transfer function fit of the response.
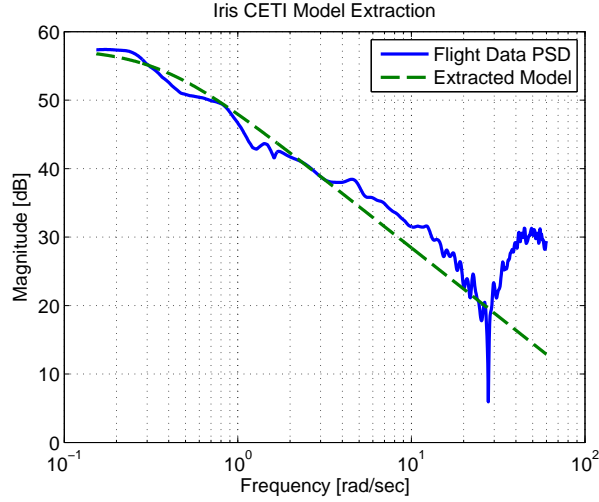
Fig. 17. Extraction of a CETI model in the longitudinal axis from flight data

$$G_{\delta_t}(s) = \frac{264}{s + 0.351} \qquad (8)$$

This transfer function represents the control equivalent turbulence input for the turbulence level from flight. The fit tracks well up to around $\omega = 4$ rad/sec and is consistent with the first-order of the CETI model given in Refs. 5, 6.

The extracted CETI autospectrum is nearly identical to the ones generated during the simulation analysis. Impacts from the control system and noise are seen near the crossover frequency just as they were in simulation. This figure also shows robustness to variations in the control laws since the extracted CETI model from flight data has the same shape as in simulation even though the control systems were different.

SAMPLE APPLICATION OF CETI MODEL

The CETI model developed has two primary uses.

- Direct control system design in the frequency domain. There is no need to run time marching simulations to determine the effects of flying in turbulence. Quantities like aircraft attitude or position RMS due to varying levels of turbulence can be directly calculated in the frequency domain.

- Real-time simulation, piloted or not, to assess the aircraft response in turbulence. For a piloted aircraft, handling quality ratings could be taken in varying levels of turbulence.

In this sample application, two control systems will be simulated and compared to each other and flight data taken in the stock onboard "Stabilize" mode in both the frequency and time domains. The first control system is the same as
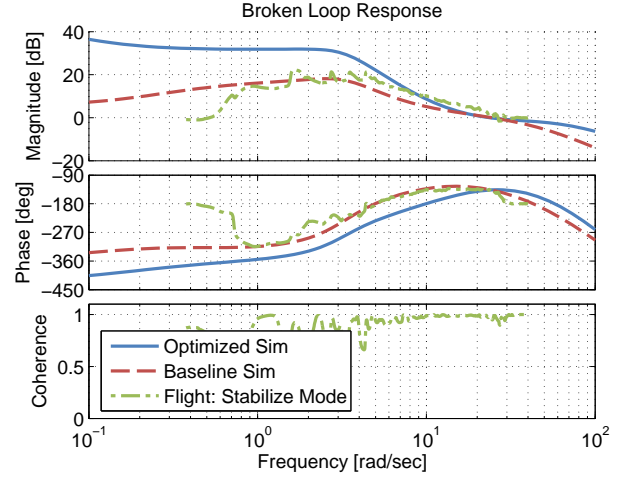

Fig. 18. Comparisons of the broken-loop response of two different Iris control systems and flight data

was used in the simulation analysis. This *optimized* control system has been tuned to have a high crossover frequency and high disturbance rejection bandwidth. An additional *baseline* control system was designed that more closely resembles the stock Iris "Stabilize" control system, and should perform worse than the more optimized one. The turbulence levels will be forced to be the same in simulation as in flight by using the identified CETI model of Eqn. (8). An output noise level giving a signal-to-noise ratio of $\bar{\sigma}_{q_m} = 2.6$ was used in simulation to match the flight data, and 300 second time simulations were generated.

Figure 18 shows the comparison of the broken loop response for the two control system in simulation as well as flight data using the stock "Stabilize" mode. While both have similar crossover frequencies, the optimized control system has much higher magnitude at low frequency, meaning the control system is more active at attenuating turbulence than the baseline control system at those frequencies. Also, the flight "Stabilize" mode data and baseline control system are very similar and so should behave similarly in the presence of turbulence.

Figure 19 shows the disturbance rejection plot for disturbances to measured aircraft pitch attitude. The baseline control system and the stock "Stablize" mode do not attenuate disturbances to as high a degree as the optimized one below the bandwidth frequency. The baseline control system has the lowest disturbance rejection bandwidth (DRB), while the optimized and "Stabilize" mode have high DRBs.

Figure 20 shows the pitch rate autospectra of the flight data and the two control systems in the example. The flight data has a slightly higher pitch rate response to turbulence than the baseline control system. The similarity between the flight test data and baseline control system was anticipated by the similarity of the broken-loop response. As was seen in the disturbance rejection figure, the optimized control system does an excellent job at rejecting the turbulence
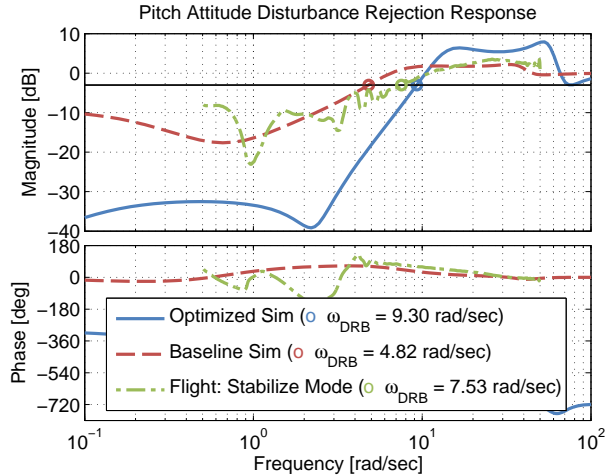
Fig. 19. Comparison of pitch attitude disturbance rejection response of two different Iris control systems

Table 2. RMS values of pitch rate due to turbulence from simulation and flight data between 0.3 and 30 rad/sec

|	Pitch Rate RMS [deg/sec]
Optimized Simulation	2.72
Baseline Simulation	3.90
Flight in "Stabilize" mode	5.15

levels, however there is a peak above 50 rad/sec. RMS values are taken between 0.3 and 30 rad/sec and are given in Table 2. This table quantifies the trends seen in the plot of the pitch rate autospectra as well as the disturbance rejection and broken loop figures. The optimized control system produces about half the RMS as the stock "Stabilize" mode.

To get a better sense for the oscillation that can be seen in flight, the pitch attitude is plotted for 20 seconds in Fig. 21. The flight data shows larger low frequency oscillations which are similar to the baseline controller. The optimized controller has small, high frequency excursions from the trim pitch attitude.

This sample application showed that the CETI model is clearly able to reproduce an accurate turbulence level for the Iris. Additionally, frequency domain metrics such as signal RMS are able to capture the predicted trends in aircraft response due to turbulence.

TOWARDS A GENERALIZABLE TURBULENCE MODEL

In addition to the CETI model carried through the sample application, an additional outdoor set of time histories were taken on a less windy day. A set of data was also taken indoors to provide a baseline. Since actual wind data was not available, the resulting autospectra can only be compared to each other, and cannot be associated with specific turbulence levels. The autospectra for the two outdoor days
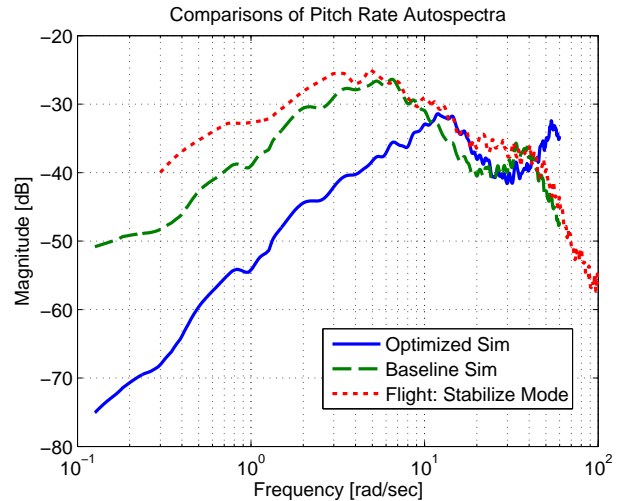
Fig. 20. Comparisons of pitch rate PSD in CETI turbulence between two simulated control systems and flight data

and the indoor data set are shown in Fig. 22. All three autospectra have the same characteristic first order form at low frequency and are separated only by a gain, K.

$$G_{\delta_t}(s) = \frac{K}{s+a} \quad (9)$$

In future work the gain and break frequency will be a function of turbulence RMS, mean velocity, or a length scale as in Ref. 5. Multiple quadrotors of varying sizes will be tested to develop length scales suitable for this configuration and make the CETI model generic. The turbulence levels will also be directly measured using an anemometer, and a larger array of turbulence data will be collected.

CONCLUSIONS

This work described and validated a methodology to extract a control equivalent turbulence input (CETI) model from closed-loop flight of a quadrotor UAS in turbulence. The key conclusions from this paper are:

1. A CETI model may be extracted from closed-loop flight test. The extraction process is effective for a control system crossover frequency that is well above the CETI dynamics.

2. Time histories greater than 200 seconds and signal-to-noise ratios $\bar{\sigma}_{q_m} > 2.5$ are needed to extract an accurate CETI model. This required signal-to-noise ratio was obtained even for the low-cost sensors that are used in the Iris.

3. The methodology is robust to plant modeling uncertainty in the Iris. A cost difference of $\Delta J < 5$ was obtained for all variations of 2σ perturbations to the bare-airframe parameters.
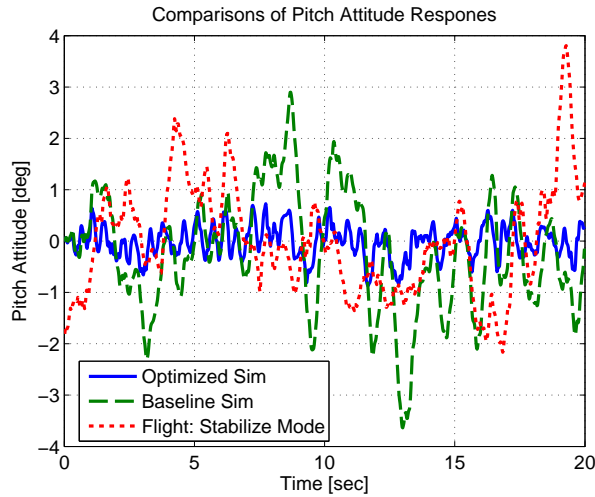
Fig. 21. Comparisons of pitch attitude time histories between two simulated control systems and flight data
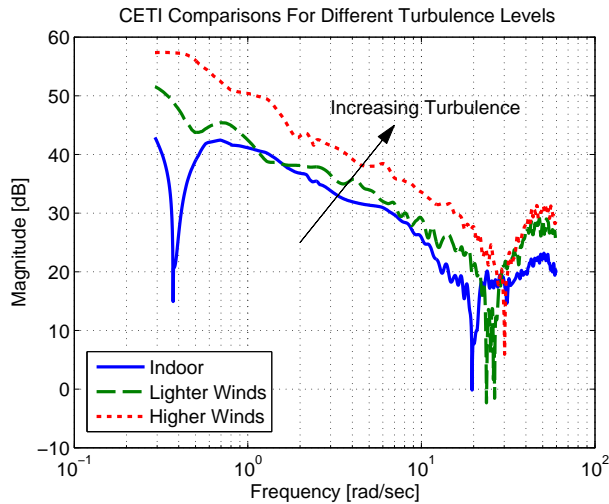
Fig. 22. Comparisons of CETI autospectra in different outdoor wind conditions as well as indoors

4. Using flight extracted noise levels and similar length time histories, a simulation was able to produce the shape of the extracted CETI autospectrum as seen in flight test.

5. A sample application verified that the CETI model produces realistic levels of turbulence in the time domain. A control system similar to the one on-board the Iris generated nearly the same oscillations as were seen in flight.

REFERENCES

[1]Tischler, M. B. and Remple, R. K., *Aircraft and Rotorcraft System Identification: Engineering Methods with Flight Test Examples*, AIAA, 2nd ed., 2012, Reston, VA.

[2]Klein, V. and Morelli, E. A., *System Identification: Theory and Practice*, AIAA, 2006, Reston, VA.

[3]Wei, W., Cohen, K., and Tischler, M. B., "System Identification and Controller Optimization of a Quadrotor UAV," American Helicopter Society 71st Annual Forum Proceedings, May 2015, Virginia Beach, VA.

[4]Niermeyer, P., Raffler, T., and Holzapfel, F., "Open-Loop Quadrotor Flight Dynamics Identification in Frequency Domain via Closed-Loop Flight Testing," Paper AIAA 2015-1539, AIAA SciTech Proceedings, January 2015, Kissimmee, FL.

[5]Lusardi, J. A., Tischler, M. B., Blanken, C. L., and Labows, S. J., "Empirically Derived Helicopter Response Model and Control System Requirements for Flight in Turbulence," *Journal of the American Helicopter Society*, July 2004, pp. 340–349.

[6]Lusardi, J. A., vonGruenhagen, W., and Seher-Weiss, S., "Parametric Turbulence Modeling for Rotorcraft Applications: Approach, Flight Tests and Verification," Rotorcraft Handling Qualities Conference, November 2008, Liverpool, UK.

[7]She, J. H., Fan, M., Ohyama, Y., Hashimoto, H., and Wu, M., "Improving Disturbance-Rejection Performance Based on Equivalent-Input-Disturbance Approach," *IEEE Transactions on Industrial Electronics*, Vol. 55, No. 1, January 2008, pp. 380–389.

[8]Cheung, K. K. et al., "An Overview of the US Army Aviation Development Directorate Quadrotor Guidance, Navigation, and Control Project," To be presented at American Helicopter Society 73rd Annual Forum, May 2017, Fort Worth, TX.

[9]Bendat, J. S. and Piersol, A. G., *Random Data: Analysis and Measurement Procedures*, John Wiley and Sons, Inc., 2nd ed., 1986, New York, NY.

[10]Berrios, M. G. et al., "Performance-Based Disturbance Rejection Criteria for Small-Scale UAS/Quadrotor with Flight Test Results," To be presented at American Helicopter Society 73rd Annual Forum, May 2017, Fort Worth, TX.

[11]Ivler, C. M., Mansur, H. M., Morford, Z. G., Kalinowski, K., and Knapp, M. E., "Flight Test of Explicit and Implicit Rotor-State Feedback Fly-By-Wire Control Laws," American Helicopter Society 72nd Annual Forum Proceedings, May 2016, West Palm Beach, FL.